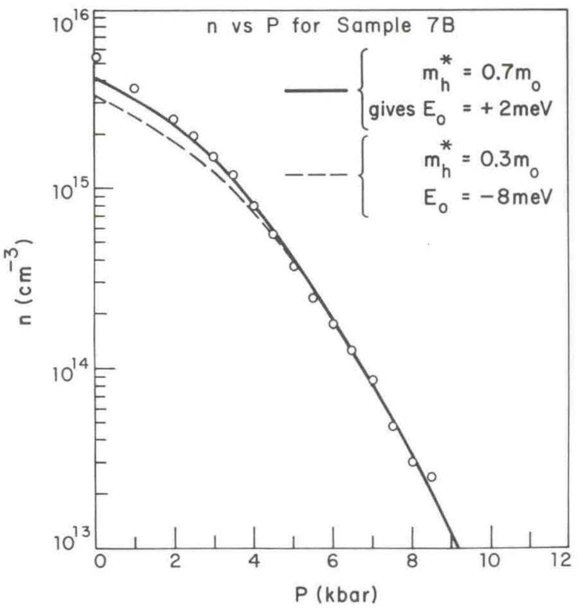

FIG. 5. Number of electrons in sample 7B as a function of pressure. The points are the values of n deduced from the experimental data. The lines are calculated from the Kane's $\vec{k}\cdot\vec{p}$ model with $P_K = 8.4\times10^{-8}$ eV/cm, $\alpha = dE_g/dP = 7.0\times10^{-6}$ eV/bar.

kbar), R is constant initially and then shows strong quantum effects but remains negative. The resistivity rises very rapidly with transverse magnetic field from 0.03 Ω cm to more than 80 Ω cm at 20 kG. At high fields the Hall angle was less

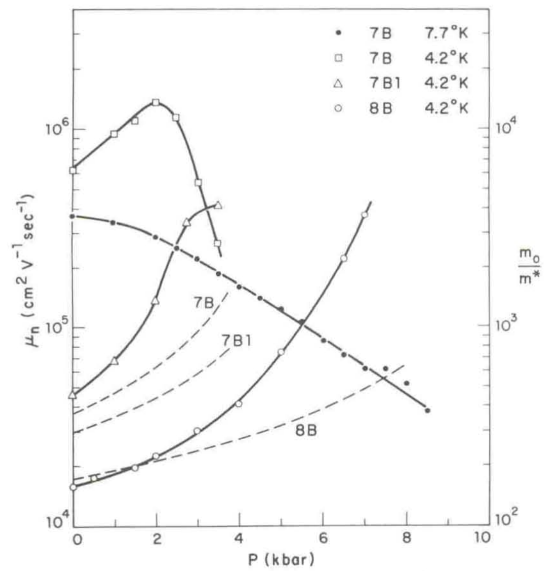

FIG. 6. Electron mobility as a function of pressure for the three samples. The variation of the reciprocal effective mass due to the change in E_g is shown by the dashed lines for comparison. The mobility is seen to increase faster than $1/m^*$ at low pressure, and for sample 7B at 4.2 °K to turn downward above 2 kbar.

TABLE I. Values for the carrier concentrations and mobilities at atmospheric pressure.

		77 °K, $P=0$				4.2 °K, $P=0$			
Sample	x	p (cm^{-3})	μ_p (cm^2 V^{-1} sec^{-1})	n (cm^{-3})	μ_n (cm^2 V^{-1} sec^{-1})	p (cm^{-3})	μ_p (cm^2 V^{-1} sec^{-1})	n (cm^{-3})	μ_n (cm^2 V^{-1} sec^{-1})
7B	0.149 ± 0.005	1.5×10^{16} ($P>5$ kbar)	450 ($P>5$ kbar)	5.3×10^{15}	3.7×10^{5}	...	...	3.4×10^{14}	6.3×10^{5}
7B1	0.149 ± 0.005	6.3×10^{17}	174	3.0×10^{15}	3.2×10^{4}	1.5×10^{17}	76	8.8×10^{14}	4.6×10^{4}
8B	0.138 ± 0.005	8.3×10^{17}	168	4.8×10^{15}	2.5×10^{4}	7.6×10^{17}	78	3.2×10^{15}	1.6×10^{4}

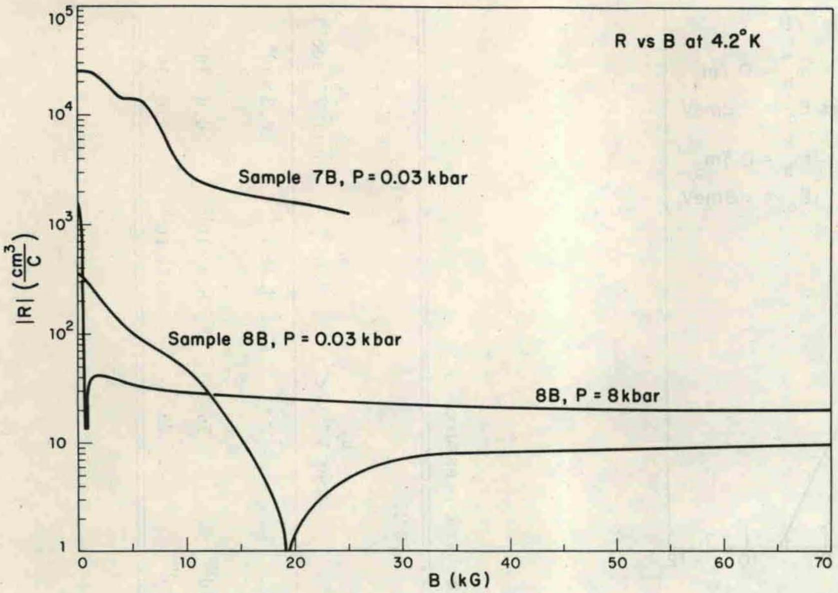

FIG. 7. Measured Hall coefficient vs magnetic field for samples 7B and 8B. R_H is negative for 7B and at low fields for 8B. The structure in the curve for sample 7B is thought to be due to quantum effects.

than 5×10^{-4} rad and we were unable to determine R owing to contact misalignment. For sample 8B at 8 kbar, the positive Hall coefficient decreases with magnetic field, falling to a value of approximately one-half its maximum value at 1.5 kG. Similar behavior was observed at 77 °K for samples 7B1 and 8B, but not for 7B, where the positive R was independent of magnetic field. The values for p quoted in Table I are obtained from the limiting value of R in strong fields.

The electron concentration and mobility for sample 7B at 4.2 °K have been obtained directly from $R(0)$ and $\sigma(0)$ since $\sigma_n(0) \gg \sigma_p(0)$, while the carrier concentrations and mobilities for samples 7B1 and 8B were obtained by using the method of the Appendix. The electron concentrations and mobilities for all three samples are shown as a function of pressure in Figs. 6 and 8. The hole concentrations and mobilities for sample 7B1 and 8B at zero pressure are given in Table I. The hole concentrations fall by approximately 40% between 0 and 9 kbar.

Longitudinal magnetoconductivity measurements were made on all three samples at helium temperatures at a series of fixed pressures. Some typical results are shown in Fig. 9. Shubnikov–de Haas oscillations were observed in many cases in the low-field region; see, for example, the $P=0$ curve of Fig. 9(b). The oscillations were observed for sample 8B at pressures up to 5 kbar [although they cannot be seen on the compressed scale of Fig. 9(a)]. The electron concentrations obtained from the periods of the oscillations in this sample are plotted in Fig. 8. These electron concentrations obtained at zero pressure for samples 7B and 7B1 are in good agreement with the concentrations obtained from the Hall data. Measurements were made on sample 8B at 77 °K, and here the conductivity was observed to change by a factor of 2 at low pressures, the change occurring

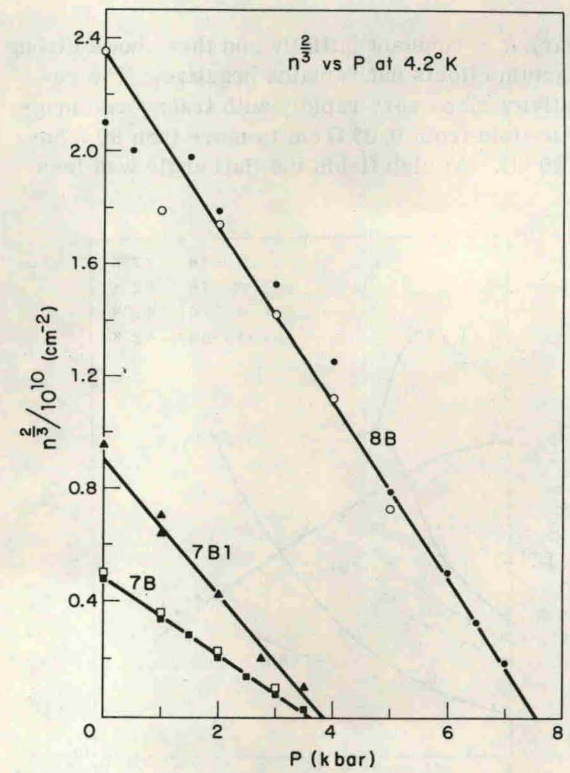

FIG. 8. Plot of the $\frac{2}{3}$ power of the electron concentration vs pressure at 4.2 °K for the three samples. The straight lines are calculated from the $\vec{k}\cdot\vec{p}$ theory. The open and solid squares for sample 7B indicate the results from two specimens. For sample 8B the open circles represent $n^{2/3}$ deduced from Shubnikov–de Haas results and the solid circles from Hall data.